Solvent Effects on Horse Apomyoglobin Dynamics†

Ahmed Haouz,‡ Jean-Marie Glandieres,‡ Christian Zentz,‡ Serge Pin,‡ Jean Ramstein,§ Patrick Tauc,|| Jean-Claude Brochon,|| and Bernard Alpert*,‡

Laboratoire de Biologie Physico-Chimique, Université Denis Diderot, 2 place Jussieu, 75251 Paris Cedex 05, France, CBM (CNRS), 1A avenue de la Recherche Scientifique, 45071 Orléans Cedex 2, France, and LURE and Laboratoire de Biochimie Moléculaire et Cellulaire, Université Paris Sud, 91 Orsay, France

Received September 9, 1997; Revised Manuscript Received December 12, 1997

ABSTRACT: The effects of the solvent conditions (buffer pH 9, 8, or 7 or buffer pH 6.5 alone or mixed with 3.2% ethanol or 6.2% formamide) on the protein dynamics of horse apomyoglobin were investigated through tryptophan fluorescence quenching, spectra, and decay properties. Raising the pH (which induces discontinuous protein conformation changes) increases the structural fluctuations inside the hydrophobic A, G, and H helix core. Mixed solutions containing either 3.2% ethanol or 6.2% formamide (which redistribute water molecules on the protein surface) produce protein dynamics changes in the vicinity of the two Trp residues, without inducing particular constraints on these very residues. Formamide increases, in the same way, the polarity and the protein flexibility while ethanol reduces both. The present fluorescence work also shows that, whatever the outside solvent, the two Trp residues W7 and W14, embedded in the A, G, and H helix core, are equally and statistically reached by small molecules diffusing inside the protein matrix. Hydrogen−tritium exchange measurements on the protein in mixed solvents reveal that the dynamics of the A, G, and H helix cluster and of the B and E helixes are greatly influenced by the nature of the outside medium. A small amount of formamide in the buffer increases the protein fluctuations while an ethanol−water mixture reduces them. We suggest that the hydratation state of the protein surface could be the relevant parameter of the protein dynamics.

One of the characteristics of proteins is that their functional properties can vary with the solvent conditions (*1*−*5*). High concentrations of neutral organic solvents denature and polymerize proteins (*6*). Low amounts of these solvents do not denature proteins (*7, 8*) and, without binding the protein (*4, 9*), produce slight conformational changes via perturbation of the protein solvation surface (*10*). On the myoglobin molecule, they only lessen or increase the tensions on the hydrated β-turns (*11*). On the other hand, pH controls the hydrogen bonds between particular histidine residues of adjacent chains (*12*). The protein dynamics of myoglobin could be coupled to these structural changes. So, the aim of this paper was to investigate the possible changes in horse apomyoglobin (apoMb) dynamics due to the external medium and to see whether any known structure changes can be correlated to them. Indeed, in the absence of the heme moiety, tryptophan (Trp) fluorescence emission can probe the conformational changes and the dynamic variability of the protein (*13*−*15*). Furthermore, apoMb—in nondenaturing conditions—retains the main features of the myoglobin structure: a compact and stable hydrophobic core (the A, G, and H helix cluster) and a more disordered domain (the C, D, and F helixes) (*16*−*20*).

The external medium effects on apoMb were essentially researched in terms of flexibility changes of the protein structure, which, in turn, may generate a great variety of environments that the Trp fluorophores can experience during their excited states. Thus, fluorescence spectra, fluorescence decay times, and fluorescence quenching experiments on the two Trp residues (W7, W14), located within the A, G, and H helix cluster, have provided information on the local structural and dynamic features of this apoMb domain. More generally, since hydrogen-isotope exchange of amide and side-chain protons allows the exploration of the overall protein dynamics, the effects of low alcohol (or amide) concentrations on the apoMb dynamic properties have also been examined through the perturbations of the hydrogen exchange kinetics (*21*).

When pH reorganizes specific tertiary contacts inside this protein (*12*), or organic solvents induce particular strains on β-turns (*11*), these perturbations can produce important changes in the compactness of the bulk protein where the Trp residues are located. In this case, the protein strains should induce differences in the electronic organization of the buried Trp (*22*−*24*) and thus modify the values of the Trp limiting anisotropy. So, these possible conformation-induced electronic structure changes were sought for through the Trp fluorescence emission anisotropy coupled to its fluorescence dynamic quenching.

MATERIALS AND METHODS

Salts and Organic Solvents. Tris(hydroxymethyl)aminomethane, bis-Tris [[bis(2-hydroxyethyl)amino]tris(hy-

† This study on protein dynamics is dedicated to the memory of Professor Gregorio Weber (University of Illinois at Urbana-Champaign).

* Correspondence should be addressed to this author: Tel, 33 01 44 27 47 38; fax, 33 01 44 27 69 95; e-mail, bea@ccr.jussieu.fr.

‡ Laboratoire de Biologie Physico-Chimique.

§ CBM (CNRS).

|| LURE and Laboratoire de Biochimie Moléculaire et Cellulaire.

S0006-2960(97)02236-8 CCC: $15.00
Published on Web 02/13/1998

droxymethyl)methane], formamide, ethanol, and NATA (*N*-acetyltryptophanamide) were purchased from Sigma. All solutions were obtained by dissolving bis-Tris or Tris in bidistilled water (0.8×10^{-6} S of conductance). In the water/organic solvent mixtures, a 20 mM bis-Tris buffer, at pH 6.5, was used. The (%) molar fractions (mol of cosolvent/100 mol of solution) of formamide were 0.5%, 1.0%, and 6.2%, and the molar fractions of ethanol were 0.8%, 1.6%, and 3.2%.

Protein Preparation. Horse heart metmyoglobin was purchased from Sigma and used without further purification. Apoprotein was obtained from the holoprotein by the acid−acetone extraction technique (*25*). ApoMb samples were prepared by dissolving the lyophilized apoprotein in 20 mM bis-Tris buffer at pH 6.5 and 7, in 20 mM Tris buffer at pH 8 and 9, or in water/organic solvent mixtures (see above). The samples were centrifuged at 7 °C just before the measurements, which were carried out on the supernatant at the same temperature. ApoMb concentrations were determined by optical absorbance at 280 nm, using a molar absorption coefficient, $\epsilon = 13\,500$ M^{-1} cm^{-1} (*26*). The native form of these apoMb samples was checked by two independent experiments. First, apoMb solubilized in 20 mM bis-Tris buffer pH 6.5, when alone and when mixed with either 3.2% of ethanol or 6.2% of formamide, must give the same UV optical absorption spectrum. Since the UV spectrum is unperturbed (not shown), the spatial conformation of apoMb was assumed not to be disrupted (*27*). Second, the experimental conditions (which differ in pH or in nature of cosolvent at low concentration) must not prevent the apoprotein from rebinding the heme group in order to give the native holoprotein (*28*).

Optical Absorption and Fluorescence Measurements. UV optical absorption spectra were made on a Cary 3E recording spectrophotometer. Fluorescence emission was measured on a Perkin-Elmer LS-5B spectrofluorometer using an emission and excitation bandwidth of 2.5 nm and a cell with an optical path length of 1 cm. Trp fluorescence anisotropy was obtained with a SLM 8000 spectrofluorometer using a linear polarized excitation beam at a wavelength of 295 nm. The excitation and emission bandwidths were 2 nm. The anisotropy value was obtained from the net count above the background on the parallel and perpendicular components of the emission: the count was collected over 2 s for each component, and each count was repeated 5 times. All fluorescence intensities were obtained on samples having a concentration around 2×10^{-5} M of protein (OD $\leq$ 0.1 at 295 nm). The relative quantum yield (Q_r) of the Trp fluorescence from apoMb, solubilized in each mixed solvent, was obtained by dividing the slope of the linear variation linking the Trp emission intensity to the protein concentration (6×10^{-6} to 3×10^{-5} M) by the corresponding slope obtained when the protein was dissolved in the reference buffer.

Trp fluorescence quenching used dichloroacetamide (DCA), an apolar solute which is perfectly soluble in water and in the two organic solvents. This collisional quencher is also known to be totally efficient ($\gamma = 1$) (*29, 30*).

Fluorescence intensity decays were obtained using a single photoelectron timing method and the synchrotron radiation from the Orsay storage ring (Super ACO, LURE) as a pulsed-light source working at a frequency of 8.33 MHz. The fluorescence excitation wavelength was 300 nm with a pulse duration of 1.1 ns. All the emitted fluorescence was detected by a Hamamatsu microchannel plate R1564U-06 set at a right angle through a set of $CuSO_4$ filters, which eliminate the light scattering of the excitation beam. The light emitted by the solvent without protein was measured for each sample, for the same accumulation time, and these counts were subtracted from their respective sample decay curve. The apparatus response function was measured at the emission wavelength with a scattering Ludox solution. Time resolution was 50 ps/channel, with 2048 channels used for decay storage.

Trp fluorescence intensity decays are given by

$$F(t) = \sum \alpha_i \exp(-t/\tau_i)$$

where α_i is the pre-exponential factor and τ_i the decay time for the i^{th} emitting component. Each fractional contribution f_i ($f_i = F_i/\sum F_i$) to the total fluorescence intensity $\sum F_i = \int F(t)\,dt$ is related to its corresponding pre-exponential factor α_i and its decay time τ_i by the relationship

$$f_i = \alpha_i \tau_i / \sum \alpha_i \tau_i$$

All parameters were extracted from the experimental decay emission using the Livesay and Brochon treatment (*31*).

Currently, Trp fluorescence experiments on proteins use an average fluorescence decay time obtained by

$$\langle \tau \rangle = \sum f_i \tau_i$$

where τ_i are the observed discrete decay time values and f_i the contributions of the corresponding fluorescence intensity fractions. Only this average decay time was used in the analyses of the Trp fluorescence quenching experiments.

Tritium−Hydrogen Exchange. The kinetics of hydrogen−tritium exchange were studied by using the two gel-filtration column method (*32*). Exchange started at time $t = 0$, when the tritium-labeled apoMb was loaded onto a Sephadex fine grade G-25 column (8×1 cm), equilibrated with the corresponding nonradioactive mixed solvent.

The amount of tritium still bound at time t was determined by passing 0.3-mL aliquots from the collected protein fraction through a second Sephadex G-25 column (5×1 cm). This column removed the tritiated solvent formed during the elapsed time *t*. Four eluted fractions were collected and selected on the basis of a constant ratio between the tritium activity and the protein concentration. The tritium activity $a(t)$ of each collected fraction was measured in duplicate with an Intertechnique SL 30 scintillation counter. At each sampling time, the number of labile tritium atoms remaining unexchanged in a protein molecule was converted to the number of protons unexchanged $N(t)$ using the expression (*33*)

$$N(t) = (111/1.21)(a(t)/a_0)(1/c)$$

where a_0 is the tritium count level of the protein solution before its application to the first column. The number 111 is the proton molarity in water, and the number 1.21 corrects

Table 1: Mixed-Solvent Effects on the Apomyoglobin Trp Fluorescence Spectra[a]

mixed solvent	λ_{max}[b] (nm) (±1 nm)	$\Delta\lambda$[c] (±0.5 nm)	Q_r[d] (±5%)	$\langle\tau_0\rangle$[e] (ns)
bis-Tris 20 mM pH 6.5	334	56.5	1 (ref)	2.4
bis-Tris 20 mM pH 6.5 + 3.2% ethanol	332	55.5	1.0_3	2.1
bis-Tris 20 mM pH 6.5 + 6.2% formamide	340	60	1.1_1	3.2

[a] Temperature = 7 °C. [b] λ_{max}: wavelength of maximum fluorescence emission. [c] $\Delta\lambda$: bandwidth measured at half intensity of the maximum emission. [d] Q_r: fluorescence quantum yield relative to the Trp fluorescence intensity of horse apomyoglobin in bis-Tris buffer pH 6.5. [e] $\langle\tau_0\rangle$: mean value of the fluorescence decay time.

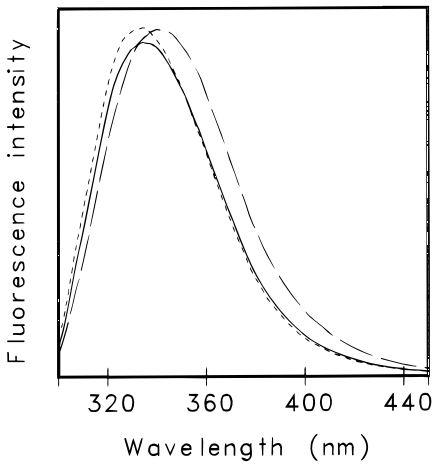

FIGURE 1: Effects of cosolvents on the tryptophan fluorescence emission of apomyoglobin at 7 °C in bis-Tris buffer (20 mM, pH 6.5): (—) buffer alone, (- - -) buffer + 3.2% ethanol, (— — —) buffer + 6.2% formamide. λ_{exc} = 295 nm. [apoMb] = 2×10^{-5} M.

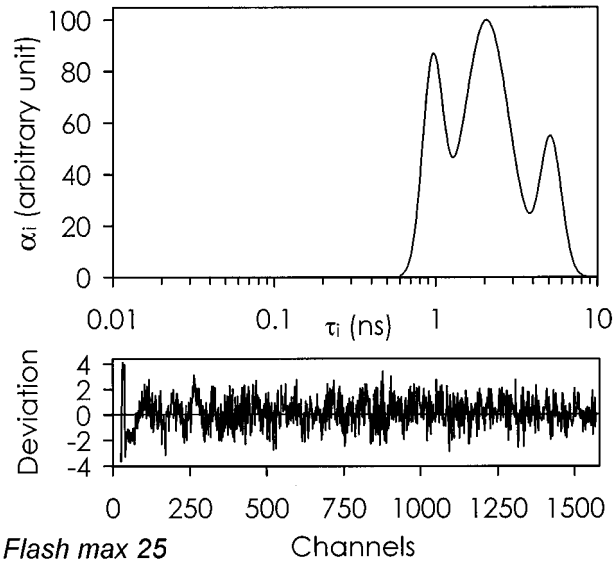

FIGURE 2: Tryptophan fluorescence decay time distribution of apomyoglobin at 7 °C in bis-Tris buffer (20 mM, pH = 6.5). The pattern gives the continuum of the pre-exponential factor α versus the fluorescence decay time τ values (in log scale). λ_{exc} = 300 nm. Pulse duration: 1.1 ns. Time resolution: 50 ps/channel.

for the preferential binding of tritium by peptide groups (*34*). *c* is the apoMb concentration in the eluted fractions.

RESULTS

Trp Fluorescence Spectra. The Trp emission spectrum of horse apoMb in buffer (pH 6.5−9) is close to that of sperm whale apoMb (*35*): there is no detectible change over this pH range. In the presence of increasing concentrations of ethanol, apoMb fluorescence shows a progressive blue shift; in the case of formamide, it is progressively red shifted. Figure 1 gives the spectra of apoMb in the buffer alone and in the presence of 3.2% of ethanol and 6.2% of formamide. Table 1 gives the fluorescence bandwidth, emission peak, and quantum yield measured for the highest cosolvent concentrations. The data show that the addition of ethanol induces a hydrophobic environment around the Trp residues and the addition of formamide induces a polar medium. NATA, under the same conditions, does not exhibit any fluorescence variation (data not shown). So, the perturbations of the Trp fluorescence from apoMb are induced by specific rearrangements of the protein surrounding these residues. These rearrangements are undoubtedly due, in turn, to different protein surface solvation states induced by the cosolvents (*10*).

Trp Fluorescence Decay Time. The fluorescence intensity decay of Trp from horse apoMb is multiexponential. The decay time distribution pattern of apoMb at pH 6.5 is presented in Figure 2. The presence of organic cosolvents and pH changes both affect this distribution. The decay time distribution of the Trp emission, however, can always be analyzed with three decay components. The intensity fractions and the decay times for these three components are collected in Table 2. Although pH reorganizes the fluorescence decay time distribution, it does not affect the mean decay time value. This could explain why the quantum yield of apoMb fluorescence does not vary significantly in this pH range (*36*). Besides, mixed solvents slightly affect the average Trp fluorescence decay time and the relative quantum yield.

The large effect on the decay time distribution (Table 2) of the Trp fluorescence intensity can be explained in terms of either dynamic relaxation or conformational heterogeneity (*37*), or both. In the case of a pH change, one could argue that the extent of protonation of nearby amino acid residues and the tertiary conformational changes induced by the bridge between histidine residues (*12*) could lead to a change in the degree of the Trp relaxation (*14, 38*). In the case of organic cosolvents, the p*K* of particular residues can be modified. Then Trp relaxation should be also involved. In addition alcohol and amide have the ability to reorganize (in an opposing way) the water content on the protein periphery (*10, 39, 40*). The number of adsorbed water molecules and the strength of the protein−water coupling (*10*) could lead to the selection of particular protein conformational substates (*38*). These states could be also involved in the Trp fluorescence decay distribution.

Trp Fluorescence Quenching Lehrer Relationship. Conformational changes in the monomeric protein, induced either by the pH or by the nature of the organic cosolvent, could modify the access to the different parts of the A helix, where

Table 2: Solvent Effects on the Trp Fluorescence Decays of Apomyoglobin[a]

	τ^b (ns)	f^c (%)	τ^b (ns)	f^c (%)	τ^b (ns)	f^c (%)	$\langle\tau_0\rangle^d$ (ns)
pH 6.5	0.96	27	2.06	51	5.16	22	2.4
pH 7	0.93	30	2.20	47	4.94	23	2.4
pH 8	0.74	26	2.27	54	5.40	20	2.4
pH 9	0.80	35	2.23	45	5.6	20	2.4
pH 6.5 + 3.2% ethanol	0.68	31	1.82	48	5.01	21	2.1
pH 6.5 + 6.2% formamide	1.12	25	2.7	47	5.93	28	3.2

[a] Excitation wavelength 300 nm, fluorescence detected through a set of $CuSO_4$ filters. Temperature = 7 °C. [b] τ: fluorescence decay time of each component. [c] f: fluorescence intensity ratio of each individual component to the total emission intensity. [d] $\langle\tau_0\rangle$: averaged fluorescence decay time. Precision: ±0.1 ns.

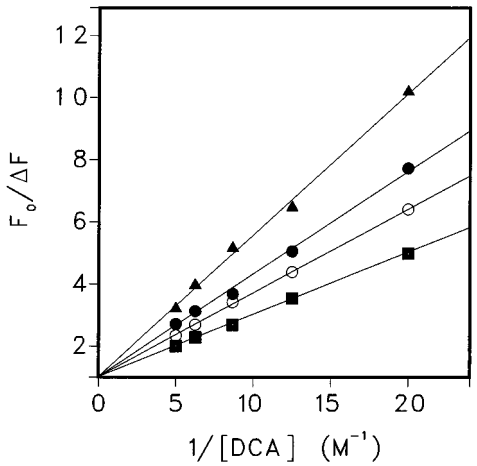

FIGURE 3: Lehrer plots of the Trp fluorescence quenching of apomyoglobin at 7 °C: (●) bis-Tris 20 mM pH 6.5 (○) Tris 20 mM pH 9 (▲) bis-Tris 20 mM pH 6.5 + 3.2% ethanol (■) bis-Tris 20 mM pH 6.5 + 6.2% formamide. All curves $F_0/\Delta F = 1/f + 1/(f\,K\,[\mathrm{DCA}])$ give the same fraction ($f = 1$) of accessible tryptophan residues. $\lambda_{exc} = 295$ nm. [apoMb] = 2×10^{-5} M.

the two Trp residues are located. Indeed, it was suggested that the W7 is more exposed than the W14, which is known to be deeply buried (*17*, *41*). Trp fluorescence quenching data as a function of DCA concentration quencher were analyzed according to the Lehrer relationship (*42*)

$$F_0/\Delta F = 1/(fK[\mathrm{DCA}]) + 1/f$$

where $\Delta F = F_0 - F$ is the fluorescence intensity decrease due to the quencher [DCA] concentration, f is the fraction of the accessible Trp residues within the protein, and K is the quenching constant of these accessible residues. Figure 3 gives the plot of $F_0/\Delta F$ vs 1/[DCA]. The $F_0/\Delta F$ axis is intercepted at $1/f$ when [DCA] $\rightarrow \infty$. The value of f is always 1, regardless of the pH or the nature of the cosolvent. This means that, irrespective of the external medium composition, DCA quencher molecules are continuously colliding with either Trp residue. So, using the slope value ($1/K$) of the Lehrer representation, encounters between DCA molecules and Trp residues of the apoMb were analyzed from the Stern−Volmer constant (*43*)

$$K = k\langle\tau_0\rangle$$

where k is the bimolecular kinetic constant of the collisional process and $\langle\tau_0\rangle$ is the average Trp fluorescence decay time in the absence of DCA quencher molecules. The value of the kinetic constant, k, increases in the presence of formamide and decreases in the presence of ethanol (Table 3). This value is also lower at pH 6.5 than at pH 9. Therefore, the protein fluctuations around the Trp residues can be either speeded up or slowed down by the outside medium around the apoMb molecule.

Trp Fluorescence Limiting Anisotropy. Linear anisotropy of indole absorption in a rigid phase indicates a possible inversion of ^1L_b and ^1L_a levels (*22*, *23*, *44*). The density and heterogeneity of bulk protein could induce specific ^1L_b and ^1L_a inversion in the Trp residues embedded within the protein (*24*). So, various protein conformational organization pathways induced by the solvent conditions might then promote electronic structure changes on the Trp residues.

To check whether the various external media induce different Trp electronic structures, the limiting anisotropy A_0 of this fluorophore was determined by the fluorescence quenching technique. When the average fluorescence decay time $\langle\tau\rangle$ decreases by collisional quenching, the fluorescence anisotropy $A(\langle\tau\rangle)$ should increase and tend to the value of the limiting anisotropy A_0, as shown by the Perrin relationship (*45*),

$$1/A = (1/A_0)(1 + \langle\tau\rangle/\rho)$$

where ρ is the protein correlation time.

The Trp fluorescence quenching being dynamic, we have $\langle\tau_0\rangle/\langle\tau\rangle = F_0/F$ (data not shown), and the Perrin relationship can be written

$$1/A = \frac{1}{A_0}\left(1 + \frac{\langle\tau_0\rangle}{\rho}\frac{F}{F_0}\right)$$

where $\langle\tau_0\rangle$ and F_0 and $\langle\tau\rangle$ and F are the mean fluorescence decay times and the fluorescence intensities in the absence and in the presence of quencher, respectively. When the DCA quencher concentration increases so that [DCA] $\rightarrow \infty$, F/F_0 tends to 0, and $1/A$ should tend to $1/A_0$.

For the buffers at pH 6.5 and 9 and also for the mixed solvents, the straight lines $1/A = f(F/F_0)$ intercept the $1/A$ axis at the same value $1/A_0$ (Figure 4). This extrapolation gives a limiting anisotropy of $A_0 = 0.24$ for the Trp in the apoMb molecule excited at 295 nm, which is equivalent to the limiting anisotropy of Trp immobilized in propylene glycol at −58 °C (*46*). Therefore the basic electronic structures of the Trp residues are not affected by the conformational and dynamic changes induced by the outside media on the apoMb molecule. The slopes of the straight lines $1/A = f(F/F_0)$ were not analyzed because many effects can be responsible for their particular values: internal flexibility, protein swelling (e.g., by more or less hydration), viscosity change, and others. Indeed, time depolarization experiments (data not shown) indicate important changes

Table 3: External Medium Effects on the Trp Fluorescence Quenching of Apomyoglobin[a]

medium	K^b (M^{-1})	$\langle\tau_0\rangle^c$ (ns)	k^d (10^8 M^{-1} s^{-1})
bis-Tris 20 mM pH 6.5	3	2.4	12.5
Tris 20 mM pH 9	3.7	2.4	15.4
bis-Tris 20 mM pH 6.5 + 3.2% ethanol	2.2	2.1	10.5
bis-Tris 20 mM pH 6.5 + 6.2% formamide	5.0	3.2	15.6

[a] Quencher = dichloroacetamide (DCA). Temperature = 7 °C. [b] K: Stern−Volmer quenching constant. Precision: ±0.15 M^{-1}. [c] $\langle\tau_0\rangle$: averaged decay time of the Trp fluorescence emission in the absence of quencher molecules. [d] *k*: bimolecular collisional kinetic constant. Precision: ±0.5 × 10^8 M^{-1} s^{-1}.

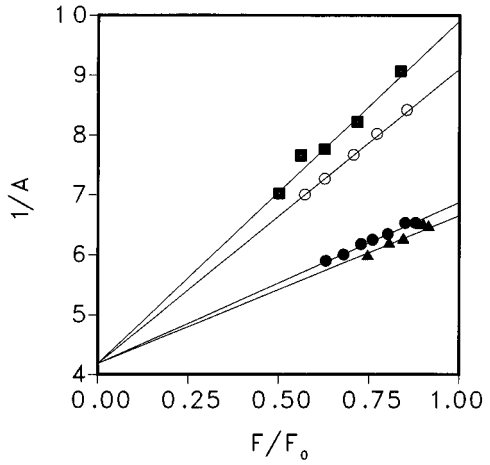

FIGURE 4: Trp fluorescence anisotropy variation of apomyoglobin at 7 °C induced by the DCA−tryptophan collisions. The curves give the Perrin plots $1/A = (1/A_0)[1 + (\langle\tau_0\rangle/\rho)(F/F_0)]$ as a function of the Trp fluorescence intensity *F*: (●) bis-Tris 20 mM pH 6.5 (○) Tris 20 mM pH 9, (▲) bis-Tris 20 mM pH 6.5 + 3.2% ethanol (■) bis-Tris 20 mM pH 6.5 + 6.2% formamide. Parallel and perpendicular Trp fluorescence intensities were measured through a WG 320 Schott filter. λ_{exc} = 295 nm. [apoMb] = 2 × 10^{-5} M.

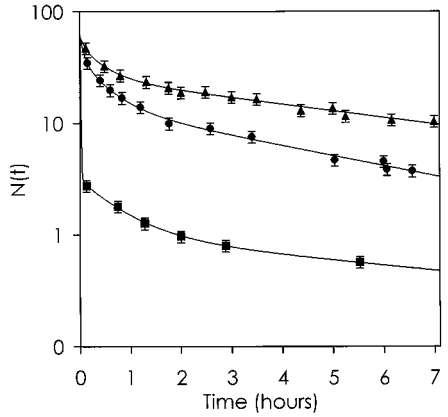

FIGURE 5: Kinetics of proton exchange of apomyoglobin at 7 °C. *N*(*t*) (plotted according to a logarithmic scale) is the number of labeled labile protons per apomyoglobin molecule remaining unexchanged at time t after mixing ^3H with ^1H. (●) bis-Tris 20 mM pH 6.5, (▲) bis-Tris 20 mM pH 6.5 + 3.2% ethanol, (■) bis-Tris 20 mM pH 6.5 + 6.2% formamide. The amount of protons still bound *N*(*t*) at each time was determined on a 0.3-mL aliquot.

both in the relaxation time for internal motions (around 1.5 ns) and in the protein time rotation (around 15 ns).

Proton Exchange. The kinetics of $^3H-^1H$ exchange in apoMb were studied over a 6-h time range. Figure 5 shows the time dependence of the $^3H-^1H$ exchange, for about 60 exchanging protons per labeled apoMb molecule. The exchange rate is very different when ethanol or formamide is added to the sample in bis-Tris buffer.

The kinetics of the proton exchange are governed by the catalytic process and the protein dynamics. Cosolvents, in amounts identical to those in the present apoMb study, did not perturb the proton exchange behavior of the holoprotein (*11*); so the two cosolvents do not induce catalytic processes which would be responsible for the kinetic variations observed on apoMb. This indicates the actuality of the changes in protein dynamics. We must note here that these dynamics are only observed on the protons located in the A, B, E, G, and H helixes (*16*).

The kinetics of the $^3H-^1H$ exchange can be approximated by three exponentials, reflecting at least three classes of protons (see Table 4). At pH 6.5, the fastest has a half-time (θ_1) around 3.3 min, the intermediate a half-time (θ_2) around 21.6 min, and the slowest a half-time (θ_3) around 3.3 h. The fastest process reflects the protons exchanged on the protein surface, and the slowest, the protons located in buried protein domains (*47*). For this reason, the proton exchanges of the protein surface should be most affected by the solvent nature. Formamide highly affects the proton exchanges on the protein surface, since only 3 out of the initial 60 protons remain just after the dead time. Ethanol, on the contrary, principally affects the proton exchanges in the protein core since the very labile proton exchange involves only a few protons (11 out of the 60 labeled). The kinetics of the slowly exchanging protons are also more or less modified: ethanol sharply decreases their speed (half-time $\theta_3 \cong 5$ h), and the formamide effect cannot be correctly estimated because of the few protons (1 in 60) involved. These least labile protons, most likely involved in the organization and the protein structure conservation, are exchanged only after a great number of protein fluctuations. In fact, individual proton exchanges occur very rapidly. Only the low frequency of the actual exchange gives the slow macroscopic exchange rate. In addition, proton exchanges in buried protein sites require random migration of catalysts up to this site. This migration is mediated by the fluctuations of the mobile parts of the protein (*47*, *48*). Thus, the external medium has the ability to modulate these multiple dynamic effects. So, it appears that formamide essentially increases the fluctuations of the protein shell while ethanol also reduces the motions of the protein core as well.

DISCUSSION

The hydrophobic A, G, and H helix core, where the two Trp residues (W7 and W14) are located, is one of the most protected areas in horse apoMb (*16*). As a consequence, when apoMb is subjected to solvent perturbation, the compactness of this domain (revealed by the limiting Trp fluorescence anisotropy) appears largely preserved. Me-

Table 4: Mixed Solvent Effects on the Proton Exchange of Apomyoglobin[a]

	A_1[b] (H/mol)	θ_1 (min)	A_2[b] (H/mol)	θ_2 (min)	A_3[b] (H/mol)	θ_3 (h)
bis-Tris pH 6.5	23	3.3	23	21.6	14	3.3
bis-Tris pH 6.5 + 3.2% ethanol	11	4.0	23	19.5	26	5.0
bis-Tris pH 6.5 + 6.2% formamide	57	<1	2	33	1	≅6

[a] The kinetics of the proton exchange is approximated by three exponentials $\sum_i A_i \exp(-t/\tau_i)$. The τ_i values are the decay time; here we use θ_i for the half-time of proton exchange. [b] A_i: number of labeled labile protons per apomyoglobin (H/mol). Temperature = 7 °C.

chanical constraints, which disrupt or connect a few stable domains, only affect the tertiary structure (*12*). Though the two Trp residues embedded in this domain are highly protected, both can be reached by the DCA molecules which cross this cluster during their random migration through the protein. The kinetic constant of the collisional process with the Trp residues increases with increasing pH. The apoMb charge variation is 6.6 from pH 9 to 6 and is essentially attributable to the titration of the imidazolium groups (*49*). The variation of pH also induces discontinuous protein conformation changes (*12*). At a given pH, the tertiary structure and the net charge borne by the macromolecule result from the number and the location of the imidazolium groups at particular sites of the protein. So, each value of the collisional rate constant between the DCA and the Trp residues should be linked to the particular spatial organization of the charged histidine residues (*50, 51*). In other words, the dynamics of the protein moiety around the Trp residues appear to be dependent on the charge distribution within the protein.

Establishment and disruption of the hydrogen bonding are among the most important parameters in protein dynamics (*52*). So, the dual character of the H-bond (dipole and intermolecular distance) should play a key role in these protein fluctuation changes. The dipolar character of the H-bonds in the protein could explain why the protein dynamics are sensitive to the charge distribution in the protein matrix. This could explain how the speed of the random migration of the apolar DCA quencher molecules into the highly organized core structure can vary with the pH conditions. For solutions containing either ethanol or formamide, the collisional kinetic constant value is also strongly affected. Moreover, fluorescence emission spectra show that mixed solvents modulate the hydrophobicity and the polarity of the Trp vicinity. Ethanol reinforces the hydrophobic character of this protein domain while formamide increases its polarity. These effects should also result from a new charge distribution both on and in the protein. The increase (or decrease) in polarity and the increase (or decrease) in mobility appear to be linked. Here, the dipolar character of the H-bonds in the protein can also explain how the dynamics and the polarity of the protein matrix around the Trp residues vary in the same way. The weaker and fewer the H-bonds are, the higher the protein mobility should be. This relationship offers an explanation for the modulation of the interconversion rates of the protein conformational substates (*38, 53*) reflected in the Trp fluorescence decay time.

Possible H-bond distance variations in the protein could also accompany the outside medium condition changes. The hydrogen exchange kinetic curves reveal the exchanging protons of these internal protein H-bonds (*16*). Although the kinetics of $^3H-^1H$ exchange is higher in the apoMb molecule compared to that of myoglobin (*20*), the protection factor pattern in myoglobin is also largely preserved in apoMb (*16*). Protected exchanging protons of apoMb are known to be located in the B and E helixes and in the A, G, and H helix cluster (*16*) where the Trp residues are also embedded. Proton exchange on these sites depends to a large extent on solvent accessibility and on the degree of protein structure fluctuations (*33, 54*). When the protein is in the presence of formamide, the fast exchanging time of the protons, indicates that very labile H-bonds are present (*52, 55*) and that the apoMb has a more fluctuating structure. Ethanol gives the opposite result. So, the degree of H-bond binding within the protein would be one important parameter in the structural flexibility (*52, 55*). By reorganizing the protein's peripheral water structure, though in opposite ways (*10, 39, 40*), ethanol and formamide would modify the H-bond network within the apoMb molecule.

Thermodynamic experiments on the stabilizing effect of solvents on proteins have shown the role of the preferential hydration (*10*). Corresponding measurements on protein dynamics have not been performed yet. Several studies have suggested that the dynamic properties of proteins could be coupled to the viscous properties of the bulk solvent (*56, 57*). Correlations between protein and solvent movements have also been suggested (*58*). Our experimental data concerning the solvent effects on the dynamics of the apoMb molecule point toward the contribution of the H-bonds to protein−solvent interactions. This effect could account for the protein flexibility variations and the relaxation variations around the Trp residues. So the network of water molecules around the protein (*10, 59, 60*) could be responsible for the steric and dynamic changes induced by the outside protein medium. Indeed, by changing the solvation states of the protein surface, the external medium could redistribute the strength and the number of the hydrogen bonds of the protein and in turn modify the local polarities: this would also facilitate the rearrangement of mobile parts of the protein (*48*). Dynamic changes of the monomeric apoMb, induced by either the pH or the presence of organic cosolvents, always seem to be associated with some protein matrix variations rather than with the viscous properties of the outside medium (*55*). Thus the present work strongly suggests the role of the preferential hydration of the protein surface on the protein dynamics. This solvation effect may initiate the molecular mechanism underlying the dynamic changes.

ACKNOWLEDGMENT

We are very much indebted to technicians and engineers of the synchrotron at LURE and the Linear Accelerator Laboratory (Orsay, France) for running SuperACO.

REFERENCES

1. Bohr, C., Hasselbach, K., and Krogh, A. (1904) *Skand. Arch. Physiol. 16*, 402−412.

2. Cordonne, L., Cupane, A., San Biagio, P. L., and Vitrano, E. (1979) *Biopolymers 18*, 1975−1988.
3. Schuster, S. M. (1979) *Biochemistry 18*, 1162−1167.
4. Dreyfus, M., Fries, J., Tauc, P., and Herve, G. (1984) *Biochemistry 23*, 4852−4859.
5. Ragone, R., Colonna, G., Bismuto, E., and Irace, G. (1987) *Biochemistry 26*, 2130−2134.
6. Margoliash, E., and Lustgarten, J. (1962) *J. Biol. Chem. 237*, 3397−3405.
7. Herskovits, T. T., and Jaillet, H. (1969) *Science 163*, 282−285.
8. Cassatt, J. C., and Steinhardt, J. (1971) *Biochemistry 10*, 3738−3742.
9. Lehmann, M. S., and Zaccai, G. (1984) *Biochemistry 23*, 1939−1942.
10. Timasheff, S. N. (1993) *Annu. Rev. Biophys. Biomol. Struct. 22*, 67−97.
11. Glandières, J. M., Calmettes, P., Martel, P., Zentz, C., Massat, A., Ramstein, J., and Alpert, B. (1995) *Eur. J. Biochem. 227*, 241−248.
12. Yamamoto, Y. (1997) *Eur. J. Biochem. 243*, 292−298.
13. Anderson, S. R., Brunori, M., and Weber, G. (1970) *Biochemistry 9*, 4723−4729.
14. Lakowicz, J. R., and Weber, G. (1973) *Biochemistry 12*, 4171−4179.
15. Eftink, M. R., and Ghiron, C. A (1975) *Proc. Natl. Acad. Sci. U.S.A. 72*, 3290−3294.
16. Hughson, F., Wright, P., and Baldwin, R. (1990) *Science 249*, 1544−1548.
17. Cocco, M. J., and Lecomte, J. T. J. (1990) *Biochemistry 29*, 11067−11072.
18. Barrik, D., and Baldwin, R. L. (1993) *Protein Sci. 2*, 869−876.
19. Cocco, M. J., and Lecomte, J. T. J. (1994) *Protein Sci. 3*, 267−281.
20. Johnson, R. S., and Walsh, K. A. (1994) *Protein Sci. 3*, 2411−2418.
21. Gregory, R. B., and Rosenberg, A. (1986) *Methods Enzymol. 131*, 448−508.
22. Weber, G. (1960) *Biochem. J. 75*, 335−345.
23. Zimmerman, H., and Joop, N. (1961) *Z. Elektrochem. 65*, 61−65.
24. Ilich, P., and Prendergast, F (1991) *Photochem. Photobiol. 53*, 445−453.
25. Rossi-Fanelli, A., Antonini, E., and Caputo, A. (1958) *Biochim. Biophys. Acta 30*, 608−615.
26. Colonna, G., Irace, G., Parlato, G., Aloj, S., and Balestrieri, C. (1978) *Biochim. Biophys. Acta 532*, 354−367.
27. Perutz, M., Kilmartin, J., Nagai, K., Szabo, A., and Simons, S. (1976) *Biochemistry 15*, 378−387.
28. Coppey, M., and Alpert, B. (1975) *C. R. Acad. Sci. 281*, 183−186.
29. Froehlich, P. M., and Nelson, K. (1978) *J. Phys. Chem. 82*, 2401−2403.
30. Eftink, M. R., and Ghiron, C. A. (1981) *Anal. Biochem. 114*, 199−227.
31. Liveseay, A. K., and Brochon, J. C. (1987) *Biophys. J. 52*, 693−706.
32. Englander, S. W. (1963) *Biochemistry 2*, 798−807.
33. Englander, S. W., and Englander, J. J. (1972) *Methods Enzymol. 26C*, 406−413.
34. Englander, S. W., and Poulsen, A. (1969) *Biopolymers 7*, 379−393.
35. Kirby, E. P., and Steiner, R. F. (1970) *J. Biol. Chem. 245*, 6300−6306.
36. Postnikova, G. B., Komarov, Y. E., and Yumakova, E. M. (1991) *Eur. J. Biochem. 198*, 223−232.
37. Bismuto, E., Irace, G., and Gratton, E. (1989) *Biochemistry 28*, 1508−1512.
38. Bismuto, E., Gratton, E., Sirangelo, I., and Irace, G. (1993) *Eur. J. Biochem. 218*, 213−219.
39. Rupley, J. A. (1964) *J. Phys. Chem. 68*, 2002−2003.
40. Assarsson, P., and Eirich, F. R. (1968) *J. Phys. Chem. 72*, 2710−2719.
41. Irace, G., Balestriery, C., Parlato, G., Servillo, L., and Colonna, G. (1981) *Biochemistry 20*, 792−799.
42. Lehrer, S. S. (1971) *Biochemistry 10*, 3254−3263.
43. Stern, O., and Volmer, M. (1919) *Phys. Z. 20*, 183−193.
44. Yamamoto, Y., and Tanaka, J. (1971) *Bull. Chem. Soc. Jpn 45*, 1362−1366.
45. Perrin, F. (1926) *J. Phys. Radium 7*, 390−401.
46. Valeur, B., and Weber, G. (1977) *Photochem. Photobiol. 25*, 441−444.
47. Benson, E. S., Rossi Fanelli, M. R., Giacometti, G. M., Rosenberg, A., and Antonini, E. (1973) *Biochemistry 12*, 2699−2706.
48. Wutrich, K., and Wagner, G. (1979) *J. Mol. Biol. 130*, 31−37.
49. Le Tilly, V., Pin, S., Hickel, B., and Alpert, B. (1997) *J. Am. Chem. Soc. 119*, 10810−10814.
50. Evans, S. V., and Brayer, G. D. (1990) *J. Mol. Biol. 213*, 885−897.
51. Cocco, M. J., Kao, Y.-H., Phillips, A. T., and Lecomte, J. T. J. (1992) *Biochemistry 31*, 6481−6491.
52. Lumry, R, W., and Rosenberg, A. (1975) *Colloq. Int. CNRS 246*, 53.
53. Frauenfelder, H., and Debrunner, P. (1983) *Annu. Rev. Phys. Chem. 33*, 283−303.
54. Abaturov, L. V., Yakobashvily, N. N., Jinoria, K. S., Molchanova, T. P., and Varshavsky, Y. M. (1976) *FEBS Lett. 70*, 127−130.
55. Lumry, R. (1995) *Methods Enzymol. 259*, 628−720.
56. Gavish, B. (1978) *Biophys. Struct. Mech. 4*, 37−52.
57. Beece, D., Eisenstein, L., Frauenfelder, H., Good, D., Marden, M. C., Reinisch, L., Reynolds, A. H., Sorensen, L. B., and Yue, K. T. (1980) *Biochemistry 19*, 5147−5157.
58. Phillips, G. N., and Pettitt, B. M. (1995) *Protein Sci. 4*, 149−158.
59. Carreri, G., Giansanti, A., and Rupley, J. A. (1988) *Phys. Rev. A 37*, 2703−2705.
60. Lounnas, V., and Pettitt, B. M. (1994) *Proteins 18*, 133−147.

BI972236U